

Article

Coupled Substitutions in Natural MnO(OH) Polymorphs: Infrared Spectroscopic Investigation

Nikita V. Chukanov ^{1,2,*}, Dmitry A. Varlamov ³ , Igor V. Pekov ², Natalia V. Zubkova ², Anatoly V. Kasatkin ⁴ 
and Sergey N. Britvin ⁵ 

¹ Institute of Problems of Chemical Physics, Russian Academy of Sciences, Chernogolovka, 142432 Moscow Region, Russia

² Faculty of Geology, Moscow State University, Vorobievsky Gory, 119991 Moscow, Russia; igorpekov@mail.ru (I.V.P.); n.v.zubkova@gmail.com (N.V.Z.)

³ Institute of Experimental Mineralogy Russian Academy of Sciences, 142432 Chernogolovka, Russia; dima@iem.ac.ru

⁴ Fersman Mineralogical Museum of the Russian Academy of Sciences, Leninsky Prospekt 18-2, 119071 Moscow, Russia; anatoly.kasatkin@gmail.com

⁵ Crystallography Department, Institute of Earth Sciences, St. Petersburg State University, University emb. 7/9, 199034 St. Petersburg, Russia; sbritvin@gmail.com

* Correspondence: chukanov@icp.ac.ru

Abstract: Solid solutions involving natural Mn³⁺O(OH) polymorphs, groutite, manganite, and feitknechtite are characterized and discussed based on original and literature data on the chemical composition, powder and single-crystal X-ray diffraction, and middle-range IR absorption spectra of these minerals. It is shown that manganite forms two kinds of solid-solution series, in which intermediate members have the general formulae (i) (Mn⁴⁺, Mn³⁺)O(OH, O), with pyrolusite as the Mn⁴⁺O₂ end-member, and (ii) (Mn³⁺, M²⁺)O(OH, H₂O), where M = Mn or Zn. In Zn-substituted manganite from Kapova Cave, South Urals, Russia, the Zn²⁺:Mn³⁺ ratio reaches 1:1 (the substitution of Mn³⁺ with Zn²⁺ is accompanied by the coupled substitution of OH⁻ with H₂O). Groutite forms solid-solution series with ramsdellite Mn⁴⁺O₂. In addition, the incorporation of OH⁻ anions in the 1 × 2 tunnels of ramsdellite is possible. Feitknechtite is considered to be isostructural with (or structurally related to) the compounds (M²⁺, Mn³⁺)(OH, O)₂ (M = Mn, Zn) with a pyrochroite-related layered structure.

Keywords: MnO(OH) polymorphs; isomorphism; solid solution; manganite; groutite; feitknechtite; IR spectroscopy; pigment; Kapova Cave; South Urals



Citation: Chukanov, N.V.; Varlamov, D.A.; Pekov, I.V.; Zubkova, N.V.; Kasatkin, A.V.; Britvin, S.N. Coupled Substitutions in Natural MnO(OH) Polymorphs: Infrared Spectroscopic Investigation. *Minerals* **2021**, *11*, 969. <https://doi.org/10.3390/min11090969>

Academic Editor: Styte M. Antao

Received: 12 July 2021

Accepted: 4 September 2021

Published: 6 September 2021

Publisher's Note: MDPI stays neutral with regard to jurisdictional claims in published maps and institutional affiliations.



Copyright: © 2021 by the authors. Licensee MDPI, Basel, Switzerland. This article is an open access article distributed under the terms and conditions of the Creative Commons Attribution (CC BY) license (<https://creativecommons.org/licenses/by/4.0/>).

1. Introduction

Manganese oxides and hydroxides, especially compounds with tunnel structures, are important materials used as pigments, ion exchangers for water purification, and cathode materials [1–7]. In this paper, we discuss the mechanisms of isomorphic substitutions in natural Mn³⁺O(OH) polymorphs and their relationships with the IR spectra.

Three polymorphs of the compound MnO(OH) are known. All of them were found in nature.

Groutite, α-MnO(OH), is an orthorhombic (space group *Pnma*) mineral with the 1 × 2 tunnel structure and unit-cell parameters *a* = 4.55–4.56, *b* = 10.47–10.70, *c* = 2.87 Å; *Z* = 4 [3,8–10]. The mineral is isostructural, with diaspore AlO(OH) and goethite Fe³⁺O(OH) and forming an isomorphous series with ramsdellite MnO₂. The crystal structure of groutite is a distorted derivative of the MnO₂ polymorph ramsdellite.

Electrochemical proton intercalation in ramsdellite results in the formation of groutite as a final reduction product via an intermediate isostructural phase (Mn⁴⁺, Mn³⁺)O(O, OH), so-called “groutellite” [11]. It was shown that under a laser beam, at a very low laser power, “groutellite” transforms into ramsdellite through the loss of H⁺ and the oxidation

of Mn^{3+} to Mn^{4+} [7]. Post et al. [12] discovered that domains of “groutellite” occur in most natural ramsdellite samples. The crystal structure of the “groutellite” variety with the composition $(\text{Mn}^{4+}_{0.5}\text{Mn}^{3+}_{0.5})\text{O}_{1.5}(\text{OH})_{0.5}$ was solved on a sample with a significant admixture of ramsdellite and a minor admixture of pyrolusite [13]. Groutite transforms into the tetragonal rutile-type MnO_2 polymorph pyrolusite upon heating in air above $300\text{ }^\circ\text{C}$ [10].

Manganite is a monoclinic (pseudo-orthorhombic) γ - $\text{MnO}(\text{OH})$ modification with the unit-cell parameters $a = 5.304$, $b = 5.277$, $c = 5.304\text{ \AA}$, $\beta = 90^\circ$; $Z = 4$ (space group $P2_1/c$ [10]) or, in the pseudo-orthorhombic cell setting, $a = 8.88$ – 8.94 , $b = 5.25$ – 5.28 , $c = 5.71$ – 5.75 \AA , $\beta \approx 90^\circ$; $Z = 8$ (space group $B2_1/d$) [10,14,15]. Manganite is the most stable $\text{MnO}(\text{OH})$ polymorph under common natural conditions [4,16,17]. This mineral is known in numerous localities.

The crystal structure of manganite is a distorted derivative of the pyrolusite structure. Partial substitution of Mn^{4+} with Mn^{3+} in pyrolusite with charge compensation by H^+ results in symmetry lowering from tetragonal to orthorhombic, with $a = 4.4609$, $b = 4.6113$, and $c = 2.7661\text{ \AA}$ for the compound $\text{Mn}^{4+}_{0.9}\text{Mn}^{3+}_{0.1}\text{O}_{1.9}(\text{OH})_{0.1}$ [3,18] and, further, to the monoclinic for manganite. The structures of all these minerals contain 1×1 channels (“tunnels”), which are too small for the incorporation of ions or water molecules.

The oxidation of manganite results in the formation of pyrolusite [10]. Pseudomorphs of pyrolusite after manganite crystals are common at the type locality of manganite—Ilfeld, Thuringia, Germany [19]. In the infrared (IR) spectrum of synthetic manganite nanorods obtained via a solvothermal method [20], relatively weak bands of H_2O molecules at 3440 and 1630 cm^{-1} are observed. These bands have been assigned by the authors of this work to adsorbed water, but partial substitution of $\text{Mn}^{3+} + \text{OH}$ for $\text{Mn}^{2+} + \text{H}_2\text{O}$ cannot be excluded.

Feitknechtite β - MnOOH is an insufficiently studied metastable phase in natural hydrothermal or supergene systems. This mineral is a hexagonal or trigonal polymorph of $\text{MnO}(\text{OH})$, which is typically formed in a mixture with hausmannite, $\text{Mn}^{2+}\text{Mn}^{3+}_2\text{O}_4$, as a result of rapid supergene oxidation of pyrochroite, $\text{Mn}(\text{OH})_2$ [21–23], whereas the slow oxidation of $\text{Mn}(\text{OH})_2$ produces only hausmannite. Synthetic “hydrohausmannite” obtained via the oxidation of $\text{Mn}(\text{OH})_2$ [24] was found to be a mixture of $\text{Mn}^{2+}\text{Mn}^{3+}_2\text{O}_4$ and/or γ - Mn_2O_3 with β - MnOOH rather than an individual single phase [22]. The structure of β - MnOOH is assumed, based on morphological and X-ray diffraction (XRD) data, to be closely related to the $\text{Mn}(\text{OH})_2$ (pyrochroite) structure [22]. According to Yang and Wang [25], almost-pure feitknechtite can be obtained as an intermediate phase of pyrochroite’s transformation to a birnessite-type Mn oxide in aqueous medium, at low pH values. However, as-synthesized feitknechtite rapidly transforms into manganite, the IR absorption bands of presumed feitknechtite at 1153 and 1084 cm^{-1} , erroneously assigned in [25] to $\text{Mn}^{3+}\cdots\text{OH}$ vibrations of feitknechtite, almost coincide with the IR bands of manganite (see below).

According to [26,27], feitknechtite is isostructural with CdI_2 and has the hexagonal unit cell parameters $a = 3.32$ and $c = 4.71\text{ \AA}$ ($Z = 1$), which are close to those of pyrochroite ($a \approx 3.33$, $c \approx 4.71\text{ \AA}$; $Z = 1$). Bricker [22] proposed the existence of a transformational (oxidation) series between $\text{Mn}(\text{OH})_2$ and β - $\text{MnO}(\text{OH})$ with a distorted brucite-related tetragonal structure and the existence of structurally related compounds $(\text{Mn}^{2+}, \text{Mn}^{3+})(\text{OH}, \text{O})_2$ with intermediate compositions and, consequently, nonequivalent situations around the OH groups. The two-stage dehydration of feitknechtite from the Noda-Tamagawa mine, Iwate Prefecture, Japan [23], is in agreement with this assumption. Natural feitknechtite samples do not contain significant amounts of cations other than Mn^{n+} , whereas an Mg-doped synthetic analogue of feitknechtite is known [28].

In numerous works on manganite-type $\text{MnO}(\text{OH})$ synthesis, feitknechtite formed as an intermediate unstable phase. Nanorods consisting of trigonal lamellae of twinned feitknechtite particles were synthesized in the reaction of reduction of MnO_4^- by $\text{S}_2\text{O}_3^{2-}$ [10].

According to powder XRD data, as-synthesized feitknechtite is unstable and transforms into manganite, forming pseudomorphs after feitknechtite nanoparticles.

Nanofibers of feitknechtite-type $\text{MnO}(\text{OH})$ were synthesized in the reaction between $\text{Mn}(\text{NO}_3)_2$ and aminoethanol in aqueous solution [29]. All peaks in the powder XRD pattern of as-synthesized $\text{MnO}(\text{OH})$ nanofibers were indexed to pure feitknechtite (JCPDS No. 18-0804), as reported in [16]. It was shown that the nanofibrous feitknechtite-type $\text{MnO}(\text{OH})$ can be efficiently converted into mixtures of manganese oxides (tetragonal phases of $\text{Mn}^{2+}\text{Mn}^{3+}_2\text{O}_4$ and MnO_2 and orthorhombic Mn_2O_3) through heating it to 400 °C. However, the strongest peaks at 621, 518, and 418 cm^{-1} in the IR spectrum of the product of the heating of feitknechtite nanofibers to 400 °C [29] correspond to hausmannite [30]. Peng and Ichinose [29] wrote that the initial feitknechtite is tetragonal and structurally related to tetragonal modifications of $\text{Mn}^{2+}\text{Mn}^{3+}_2\text{O}_4$ and MnO_2 , but this is an obvious mistake because the powder XRD data and morphological features definitively indicate that feitknechtite is trigonal. Unfortunately, no data on the IR spectrum of the products of the heating of feitknechtite at 400 °C in the range of O–H stretching vibrations (2000–3800 cm^{-1}) are provided in the cited paper. However, taking into account the fact that the complete removal of hydrogen from other $\text{MnO}(\text{OH})$ polymorphs, manganite and groutite, occurs upon heating in air at temperatures ≥ 400 °C [31,32], one can suppose that the products of the heating of feitknechtite at 400 °C do not contain OH groups.

Thus, the structures of feitknechtite, groutite, and manganite can be considered derivatives of the pyrochroite $\text{Mn}(\text{OH})_2$ layered structure, the ramsdellite MnO_2 1 × 2 tunnel structure, and the densest pyrolusite MnO_2 1 × 1 tunnel structure, respectively. This fact predetermines specific features and mechanisms of isomorphous substitutions in $\text{MnO}(\text{OH})$ polymorphs as well as their reduction and oxidation transformations.

This paper provides new data on isomorphism in natural $\text{MnO}(\text{OH})$ polymorphs mainly based on the IR spectroscopic data. A description of a mineral with the simplified formula $\text{Mn}^{3+}\text{ZnO}_2(\text{OH})(\text{H}_2\text{O})$, isostructural with manganite, is given herein.

2. Materials and Methods

Powder XRD data were collected with a Rigaku R-AXIS Rapid II diffractometer (image plate, rotating anode with microfocus optics) (Rigaku Corporation, Tokyo, Japan) using $\text{CoK}\alpha$ radiation, at the accelerating voltage of 40 kV and current of 15 mA in Debye–Scherrer geometry, camera diameter $d = 127.4$ mm and an exposure time of 15 min. The powder XRD pattern of feitknechtite was recorded using a Rigaku Oxford Diffraction SuperNova diffractometer (in microdiffraction mode with 0–360° Φ rotation scan) (Rigaku Corporation, Tokyo, Japan) equipped with a Pilatus 200K Dectris detector and an X-ray micro-source ($\text{MoK}\alpha$ radiation) with an accelerating voltage of 50 kV, beam current of 0.12 mA, beam size on the sample of about 0.12 mm, and an exposure time of 30 min. The sample-to-detector distance was 68 mm.

Single-crystal XRD studies of the groutite–ramsdellite series minerals were carried out using an Xcalibur S diffractometer (Agilent Technologies, Oxford, UK) equipped with a CCD detector ($\text{MoK}\alpha$ radiation).

Seven samples of $\text{MnO}(\text{OH})$ polymorphs and related minerals, listed below, have been investigated. All of them were characterized using IR spectra, X-ray diffraction (XRD) data and/or electron microprobe analyses.

Groutite from the Zaval’evskoe graphite deposit, Kirovohrad Oblast, Ukraine, forms lustrous black blocky flattened (lamellar or lenticular) crystals up to 1 cm across, assembled in groups or rose-like clusters. They occur in cracks of mica schist in association with calcite and baryte. The strongest reflections of the powder XRD pattern [d , Å (I , %)] are: 4.183 (100), 2.801 (32), 2.672 (34), 2.519 (21), 2.363 (64), 2.300 (15), 1.695 (26), 1.606 (17).

OH-bearing ramsdellite (“groutellite”) from the El’vor deposit, Goygol District, Azerbaijan, forms a dense subparallel aggregate of black long-prismatic crystals up to 5 mm long. The orthorhombic unit-cell parameters determined from the single-crystal XRD data are $a = 4.61(8)$, $b = 9.30(3)$, $c = 2.868(7)$ Å; $V = 123(2)$ Å³. The strongest lines of the powder

XRD pattern (d , Å (I , %)) are: 4.09 (100), 2.631 (74), 2.551 (34), 2.458 (41), 2.435 (52), 2.409 (37), 2.352 (35). The presence of Mn^{4+} in this sample can be assumed based on a lowered b parameter of the unit cell as compared to that of ramsdellite.

Intergrowths of groutite with “groutellite” from the Black Water mine, Apache Co., Arizona, USA, form pseudomorphs after prismatic crystals of ramsdellite up to 1 mm long. The strongest lines of the powder XRD pattern (d , Å (I , %)) are: 4.24 (100), 4.10 (80), 2.828 (50), 2.644 (50), 2.458 (60), 2.390 (90), 2.351 (50), 2.193 (50), 1.783 (50), 1.710 (70), 1.623 (50), 1.448 (70). The reflections with $d = 4.24$ and 4.10 Å correspond to groutite and “groutellite”, respectively. The orthorhombic unit-cell parameters of “groutellite”, determined from the single-crystal XRD data are $a = 4.556(10)$, $b = 10.73(2)$, $c = 2.898(13)$ Å; $V = 141.6(7)$ Å³.

H-free ramsdellite from Negusata Mountain, Shimoda, Sizuoka, Japan, occurs as an aggregate of randomly oriented black prismatic crystals. The sample was identified via IR spectrum and electron microprobe analysis.

Manganite from its type locality, Ilfeld, Thuringia, Germany, forms a group of black prismatic crystals up to 2 cm long. The IR spectrum of this sample coincides with the IR spectra of natural and synthetic manganite from literature sources.

Feitknechtite from the Zmeinogorskoe Mn deposit, Chebarkul’ district, South Urals, Russia, occurs as black granular aggregates, also containing rhodochrosite, nsutite, hausmannite, and manganite impurities. The associated minerals are rhodonite and tephroite. Feitknechtite was identified by the reflections with d values of 4.61, 2.63 (the strongest ones) as well as 2.35, 1.96, and 1.55 Å.

The electron microprobe analyses of all the above-listed minerals showed the presence of Mn as the only detectable component with an atomic number higher than that of oxygen.

The Zn-rich manganite-related mineral occurs as a black fine-grained aggregate. It originates from Kapova Cave (another name Shulgan-Tash Cave) of karst origin situated in the Burzyansky district, Bashkortostan, South Urals, Russia (53°2′40″ N, 57°3′50″ E). The cave has a passage length of more than 3000 m and is best known for the rock paintings of the primitive man of the Paleolithic era (about 36,400 years ago). Detailed analytical data for this mineral are given below.

In order to obtain IR absorption spectra, powdered samples were mixed with anhydrous KBr, pelletized, and analyzed using an ALPHA FTIR spectrometer (Bruker Optics, Karlsruhe, Germany) at a resolution of 4 cm^{-1} . The pellets were dried at 60 °C for 15 min before the analysis. Sixteen scans were collected for each spectrum. The IR spectrum of an analogous pellet of pure KBr was used as a reference. The accuracy of the determination of wavenumbers did not exceed 2 cm^{-1} .

Chemical analyses were carried out using a Tescan VEGA-II XMU INCA Energy 450 (EDS mode, 20 kV, 190 pA, beam size $< 5\text{ }\mu\text{m}$) (TESCAN, Brno, Czech Republic). The standards used were wollastonite for Ca, Mn metal for Mn, Zn metal for Zn, SiO_2 for Si, and LaPO_4 for P. The detection limits were (wt.%) 0.12 for CaO, 0.18 for ZnO, 0.11 for Mn_2O_3 , 0.08 for SiO_2 , and 0.12 for P_2O_5 .

3. Results

3.1. Groutite

The strongest bands in the IR spectrum of groutite (curve *a* in Figure 1), observed in the ranges of $1900\text{--}2900$, $990\text{--}1030$ and $500\text{--}610\text{ cm}^{-1}$, correspond to stretching vibrations of OH groups forming strong hydrogen bonds, $\text{Mn}^{3+}\cdots\text{O}\text{--}\text{H}$ bending (libration) modes, and $\text{Mn}^{3+}\text{--}\text{O}$ stretching vibrations, respectively. Additional weak bands in the ranges of $3300\text{--}3500$ and $1080\text{--}1150\text{ cm}^{-1}$ are due to stretching vibrations of OH groups forming relatively weak hydrogen bonds and overtones and/or combination modes related to the $\text{Mn}^{3+}\text{--}\text{O}$ stretching modes, respectively.

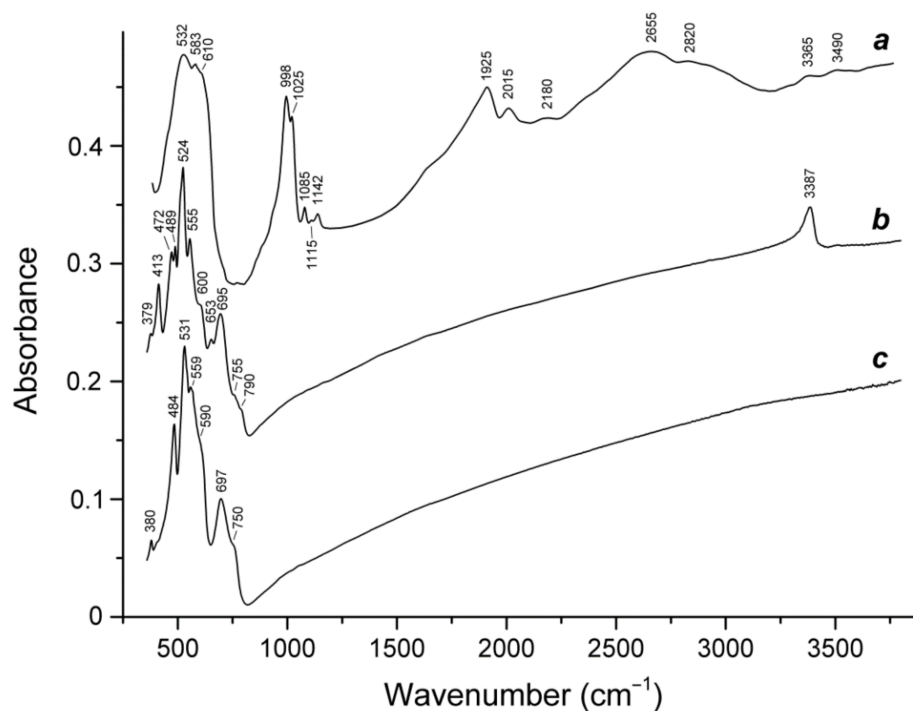


Figure 1. Infrared spectra of (a) groutite sample chemically close to the $\text{Mn}^{3+}\text{O}(\text{OH})$ end member from the Zaval'evskoe graphite deposit, Ukraine; (b) OH-bearing ramsdellite (“groutellite”) from the El'vor deposit, Azerbaijan; and (c) H-free ramsdellite Mn^{4+}O_2 from Shimoda, Japan.

There are two varieties of ramsdellite, a mineral isostructural with groutite, which are different in some features of their IR spectra. In the IR spectrum of hydrogen-free ramsdellite (curve *c* in Figure 1), only bands in the range of $360\text{--}800\text{ cm}^{-1}$, related to vibrations of the MnO_6 octahedra, were observed. In the IR spectrum of hydrogen-bearing ramsdellite (curve *b* in Figure 1), additional bands at 3387 , 653 and 413 cm^{-1} are present. These bands correspond to stretching, libration, and translational vibrations of OH groups forming relatively weak hydrogen bonds.

Kohler et al. [10] assigned the IR bands of groutite in the range of $1900\text{--}2100\text{ cm}^{-1}$ to the first overtones of bending vibrations involving OH groups (the fundamentals with the wavenumbers 990 to 1030 cm^{-1}). However, this assignment is questionable, taking into account the high intensities of these bands and the fact that anharmonic shifts for bending modes are usually positive. The statement “the real overtone positions are mostly shifted to lower wavenumbers” [10] is correct mainly for stretching modes.

Obviously, the strong and broad bands in the range of $1900\text{--}2900\text{ cm}^{-1}$ in the IR spectrum of groutite are due to O–H stretching vibrations of OH groups, forming strong hydrogen bonds. As a counter-argument to this assignment, the authors of the cited paper wrote: “A splitting amount of $\sim 600\text{ cm}^{-1}$ of the two normal modes which belong to the same internal coordinate (i.e., in-phase and out-of-phase stretching) has never been observed yet”. However, as one can see in Figure 1, this band is split into two components (an absorption maximum at 583 cm^{-1} and a shoulder at 610 cm^{-1}).

In the crystal structure of groutite, a very strong hydrogen bond $\text{O1}\cdots\text{H}\text{--}\text{O2}$ with the $\text{O1}\cdots\text{O2}$ distance of 2.62 \AA was found [10]. This value corresponds to an acid OH group. According to the correlation $\nu = 3592 - 304 \times 10^9 \cdot \exp(-d(\text{O}\cdots\text{O})/0.1321)$ between the wavenumber of O–H stretching vibrations, ν (cm^{-1}) and the distance between O atoms of an OH group and the acceptor of the hydrogen bond formed by this OH group, $d(\text{O}\cdots\text{O})$ (\AA) [33], the absorption maximum at 2655 cm^{-1} corresponds to the $d(\text{O}\cdots\text{O})$ value of 2.59 \AA , which is rather close to the value determined as a result of the structure refinement.

The corresponding O1...H distance determined from the correlation $d(\text{O}\cdots\text{H}) = 3.0897 - 0.2146 \cdot \ln(3632 - \nu)$ [33] is equal to 1.61 Å.

The absorption maximum at 1925 cm^{-1} corresponds to the $d(\text{O}\cdots\text{H})$ value of 1.49 Å, which could correspond to a virtual state of hydrogen as the H^+ cation in a local potential minimum between the O1 and O2 atoms, similar to the situation described in the model of the dynamic H atom disorder in manganite [34]. The integrated intensity of the absorptions in the range of $1800\text{--}2100 \text{ cm}^{-1}$ is about 30% of the overall integrated intensity in the O–H stretching range. Thus, the hypothetical virtual state of H^+ a local potential minimum between O1 and O2 is subordinate relative to the main state with $d(\text{O}\cdots\text{H}) = 1.61 \text{ Å}$. The splitting of the bands in the ranges of $1800\text{--}2100$ and $2300\text{--}3100 \text{ cm}^{-1}$ may be due to Fermi resonance.

No bonds of H_2O molecules (in the range of $1500\text{--}1700 \text{ cm}^{-1}$) were observed in the IR spectra of ramsdellite. For the possible role of the OH group in the ramsdellite structure, see the Discussion section. The rise of the baseline on the IR spectra in the region of higher wavenumbers is due to the strong scattering of IR radiation.

The IR spectrum of pseudomorphs after ramsdellite from the Black Water mine (Figure 2) is nearly a superposition of the spectra of groutite and OH-bearing ramsdellite. It indicates the presence of OH groups forming both weak and strong hydrogen bonds. However, the hydrogen bonds corresponding to the bands at 2695 and 2890 cm^{-1} are slightly weaker than analogous hydrogen bonds in the groutite end-member.

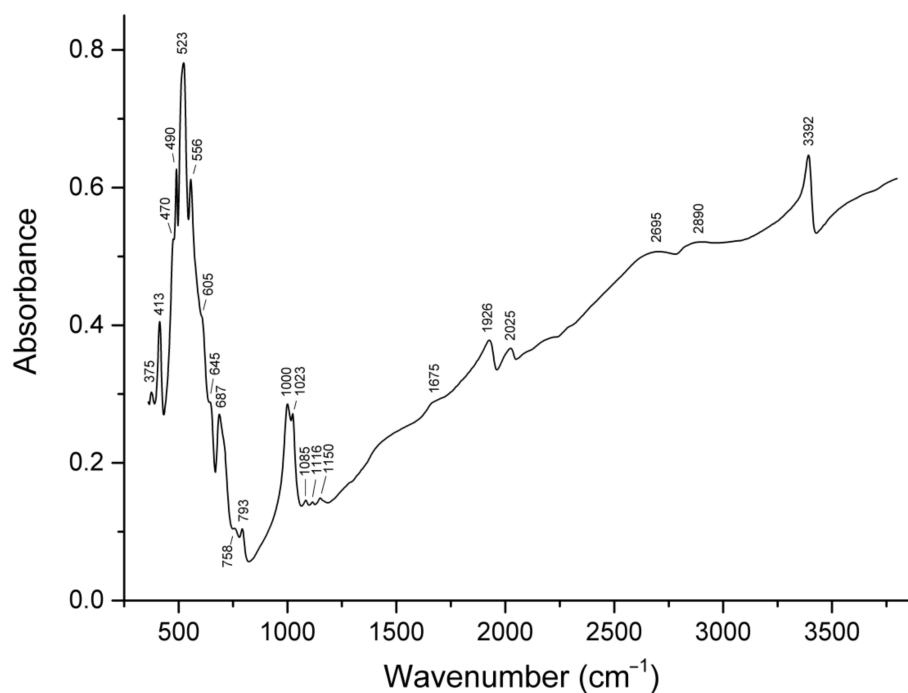


Figure 2. Infrared spectrum of two-phase (groutite + “groutellite”) pseudomorphs after ramsdellite from the Black Water mine, Arizona, USA.

3.2. Manganite

The IR spectrum of manganite from Ilfeld, Germany (curve *a* in Figure 3), is almost identical to the IR spectra of synthetic manganite, characterized using powder XRD data [4,17,35,36]. The broad absorption bands at 2010 and 2600 cm^{-1} correspond to stretching vibrations of OH groups forming strong hydrogen bonds. The distinct narrow bands at 1085 , 1114 , and 1150 cm^{-1} are due to $\text{Mn}^{3+}\cdots\text{O}\text{--}\text{H}$ bending vibrations and are considered to be characteristic bands of manganite [37]. The absorptions in the range of $400\text{--}600 \text{ cm}^{-1}$ correspond to $\text{Mn}^{3+}\text{--}\text{O}$ stretching modes, and the shoulder at 950 is an overtone or a $\text{Mn}^{3+}\text{--}\text{O}$ stretching combination mode.

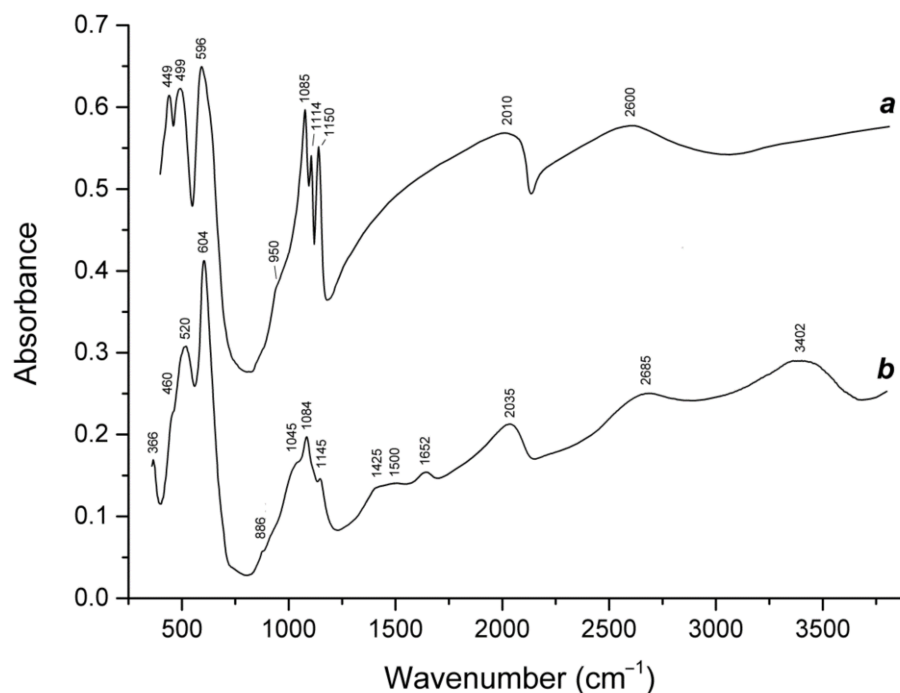


Figure 3. Infrared spectra of (a) manganite $\text{Mn}^{3+}\text{O}(\text{OH})$ from Ilfeld, Germany, and (b) Zn-rich manganite-related mineral $(\text{Mn}^{3+}, \text{Zn}^{2+})\text{O}(\text{OH}, \text{H}_2\text{O})$ from Kapova Cave, Bashkortostan, Russia.

Kohler et al. [10] assigned the band between 2000 and 2100 cm^{-1} to the first overtone of a mode related to bending vibrations of the OH group, but this assignment is very questionable, taking into account the high intensity and large width of this band. On the basis of the deviation of the OMn_3 fragments from planarity, no specific O site could be predetermined by the authors of this paper as preferred for OH. Moreover, upon deuteration, the IR bands of manganite in the ranges of 2000–2100 and 2500–2700 cm^{-1} behave differently [38], and consequently should be assigned to nonequivalent OH groups. The shifts of these bands upon deuteration undoubtedly show that they are due to O–H stretching vibrations. Taking into account the fact that the refined D–H distance of 0.98 Å in the structure of manganite is unusually long and the H···A is short (about 1.6 Å [10]), one can suppose that the presence of two bands of O–H stretching vibrations in the IR spectrum of manganite is due to the reversible transfer of the H atom from the O atom of the OH group (D) to the H-bond acceptor (A). This assumption is in agreement with the model for the dynamic H atom disorder as a result of proton tunneling in a double minimum potential of the H-bond in manganite [34]. There is no evidence for a light-stimulated tunneling process [10] but thermally stimulated tunneling cannot be excluded.

A similar set of bands was observed in the IR spectrum of the Zn, Mn-oxide from Kapova Cave (curve b in Figure 3). The ranges 2000–2700, 1000–1200, and 400–700 cm^{-1} correspond to O–H stretching (strong hydrogen bonds), M···O–H bending, and M–O stretching modes, respectively (M = Mn, Zn). Additional bands at 3402 and 1652 cm^{-1} correspond to stretching and bending vibrations of H_2O molecules forming medium-strength hydrogen bonds. The weak bands at 1425 and 886 cm^{-1} may be due to a small admixture of rhodochrosite.

The chemical composition of the mineral from Kapova Cave is given in Table 1. Only Mn, Zn and minor Ca, Si, and P impurities were detected. Thus, the charge-balanced simplified formula of the mineral is close to $\text{Mn}^{3+}_{0.5}\text{Zn}^{2+}_{0.5}\text{O}(\text{OH})_{0.5}(\text{H}_2\text{O})_{0.5}$.

Table 1. The chemical composition of the mineral from Kapova Cave (wt.%, mean of three spot analyses).

Constituent	Content	Range	Formula Coefficients *
CaO	1.18	0.57–1.67	0.02
ZnO	42.74	36.55–46.96	0.505
Mn ₂ O ₃	40.68	36.95–47.95	0.495
SiO ₂	1.54	1.34–1.86	0.02
P ₂ O ₅	1.22	1.04–1.58	0.02
Total	87.36		

Note: * The formula coefficients were calculated based on 1 Mn+Zn atom per formula unit.

The analysis of homogenized powder (CaO 1.07 wt.%, ZnO 38.55 wt.%, Mn₂O₃ 39.7 wt.%, SiO₂ 1.25 wt.%, P₂O₅ 1.06 wt.%, total 81.20 wt.%) confirmed this stoichiometry and resulted in the following empirical formula (calculated on Mn+Zn = 1): Ca_{0.02}(Mn_{0.51}Zn_{0.49})Si_{0.02}P_{0.02}(O,OH,H₂O)_x. The analytical total is lowered because the analysis was obtained from an unpolished surface.

According to the powder XRD data (Table 2), the mineral from Kapova Cave is isostructural with (or structurally closely related to) manganite. The parameters of its monoclinic unit cell calculated from the powder data are $a = 5.321(7)$, $b = 5.226(2)$, $c = 5.289(4)$ Å, $\beta = 114.45(7)^\circ$, $V = 133.9(3)$ Å³.

Table 2. Powder X-ray diffraction data (d in Å) of the manganite-related Zn,Mn-mineral from Kapova Cave.

I_{obs}	d_{obs}	d_{calc}	$h k l$
100	3.353	3.393	−111
22	2.632	2.634	−102
28	2.488	2.517	111
24	2.417	2.422, 2.407	200, 002
6	2.262	2.255	−121
7	2.201	2.230	−202
3	2.164	2.187	012
9	1.780	1.776, 1.770	220, 022
10	1.695	1.696	−222
18	1.676	1.674	−311
7	1.620	1.623	−131
10	1.500	1.489	131
9	1.439	1.436	202
7	1.321	1.325, 1.320	311, 113
7	1.231	1.237	−133

3.3. Feitknechtite

The IR spectrum of a feitknechtite-bearing aggregate (polymineralic sample from the Zmeinogorskoe deposit, South Urals, Russia) is given in Figure 4. It contains bands of rhodochrosite, manganite, and a series of bands that could be assigned to hydroxide phase(s). The IR absorption bands at 1060 and 952 cm^{−1} corresponding to Mn³⁺...O–H bending modes confirm the existence of feitknechtite [17,35,36]. Characteristic bands of other associated minerals determined using powder XRD data (hausmannite, nsutite,

rhodonite, and tephroite) were not observed. Therefore, the other bands of a hydroxide phase other than manganite are tentatively assigned to feitknechtite.

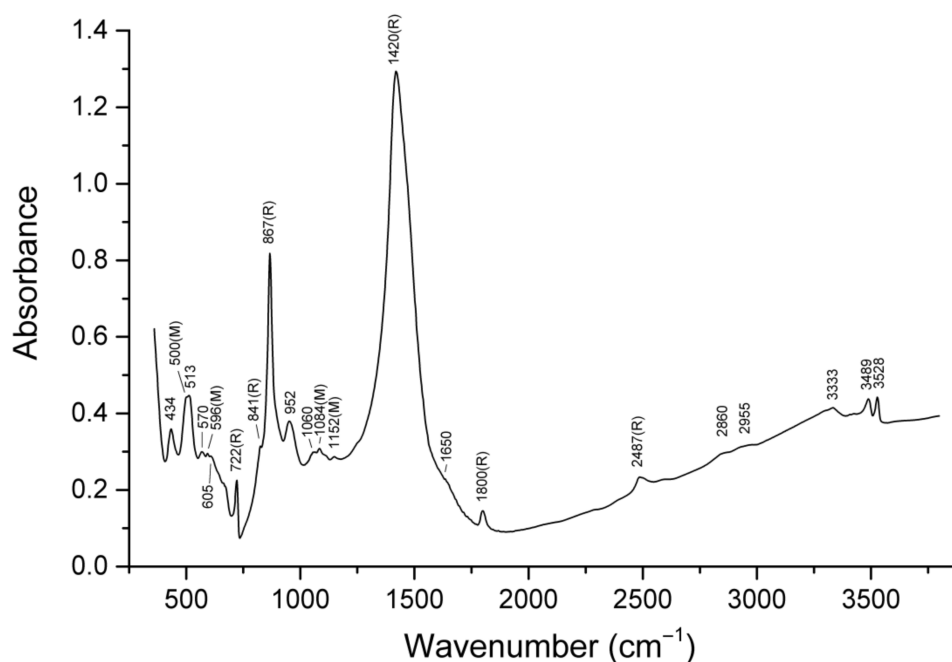


Figure 4. Infrared spectrum of a mixture of feitknechtite with rhodochrosite (R) and manganite (M) from the Zmeinogorskoe deposit, South Urals, Russia.

The bands at 3528 and 3489 cm^{-1} correspond to stretching vibrations of OH groups forming weak hydrogen bonds, which is typical of brucite-group minerals. This fact confirms the assumption of structural similarity between feitknechtite and pyrochroite. The bands at 3333 and 1650 cm^{-1} are due to water molecules, presumably intercalated in the feitknechtite structure. The nature of the weak broad absorption bands at 2955 and 2860 cm^{-1} is unclear. They may correspond to an unidentified X-ray amorphous impurity or a phase with distorted manganite structure.

4. Discussion

The nature of H-bearing species in ramsdellite is discussed by Potter and Rossman [39]. The authors of that paper wrote, “We have found that ramsdellite invariably contains a single crystallographically-ordered water” and “The intensity relationship of the bands indicate that the major hydrous species is H_2O . . . in a well-defined crystallographic site”. However, our data show that both hydrogen-free ramsdellite (curve *c* in Figure 1) and ramsdellite with admixed OH groups but without H_2O molecules (curve *b* in Figure 1) exist. The peak at 1637 cm^{-1} , corresponding to H_2O molecules in the IR spectrum of ramsdellite from Chihuahua, Mexico (Figure 5), is accompanied by the broad shoulder at ~ 3480 cm^{-1} . These bands are absent in the IR spectrum of OH-bearing ramsdellite from El’vor (curve *b* in Figure 1) and should be assigned to H_2O molecules, whereas the narrow peak at 3386–3387 cm^{-1} corresponds to OH groups. Thus, ramsdellite samples investigated by Potter and Rossman [39] contain both OH and H_2O , whereas the sample from El’vor contains only OH groups. A similar band of OH groups forming weak hydrogen bonds was observed at 3392 cm^{-1} in the IR spectrum of “groutellite” from the Black Water mine (Figure 2). The bands at 1637 and ~ 3480 cm^{-1} (Figure 5) may correspond to water molecules adsorbed by powdered mineral samples or to admixtures of hydrous minerals [40].

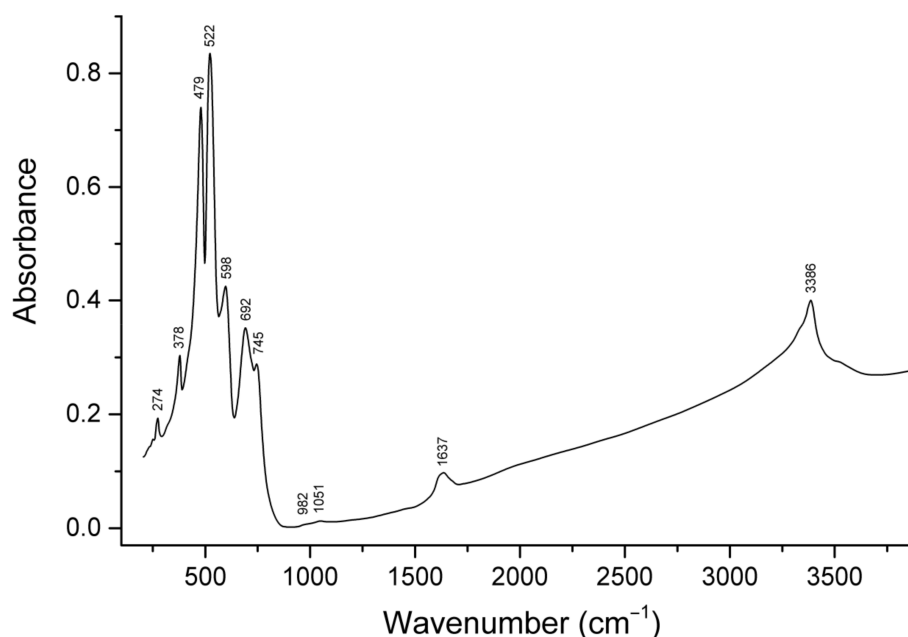


Figure 5. IR spectrum of ramsdellite from Chihuahua, Mexico, drawn using data from Potter and Rossman (1979).

The comparison of IR spectra presented in Figure 1, Figure 2, and Figure 5 shows that there may be two stages of the hydrolytic alteration of ramsdellite. In the first stage, partial protonation of the O2 atom, accompanied by partial substitution of Mn^{4+} with Mn^{3+} , takes place. According to the Libowitzki correlation [33], the product of this reaction (“groutellite” *s.s.*) is characterized by the O1...O2 distance of 2.79 Å, which is intermediate between analogous distances in the structures of groutite (2.62 Å) and H-free ramsdellite (3.23 Å). It is to be noted that the incorporation of OH^- anions and any cations (required for the charge compensation) in the 1×2 channels is impossible because of steric restrictions. On the second stage, further protonation of the O2 atom results in the transformation of the configuration of the ramsdellite framework into the topologically identical groutite framework and the formation of strong hydrogen bonds with a short O1...O2 distance (up to 2.62 Å for the groutite end-member).

Feitknechtite has been synthesized in the reaction of nanocrystalline vernadite ($\delta\text{-MnO}_2$) with aqueous solutions containing Mn^{2+} cations, at a pH below 9 [41]. It was shown [37] that in the presence of Mn^{2+} cations, transformation of a birnessite-type MnO_2 compound into manganite (*Mng*) proceeds via the intermediate unstable feitknechtite (*Ftk*) phase in accordance with the scheme $\text{Mn}^{2+}(\text{aq}) + \text{MnO}_2 + 2\text{H}_2\text{O} \rightarrow 2\text{Ftk} + 2\text{H}^+(\text{aq})$; $\text{Ftk} \rightarrow \text{Mng}$. The formation of the intermediate feitknechtite phase was faster for Zn-coprecipitated birnessite than for pure birnessite. Feitknechtite can be easily synthesized in the form of aggregates of hexagonal lamellar individuals in reactions of hexagonal birnessite-like phyllo-manganate compounds with aqueous solutions containing Mn^{2+} , at $\text{pH} \geq 7$ [17,35]. Feitknechtite is metastable and converts into manganite during aging in aqueous solution [22,42]. Thus, manganite occurring in close association with feitknechtite in the sample from the Zmeinogorskoe deposit may be a product of partial feitknechtite alteration.

Reaction with Mn^{2+} promotes the conversion of relatively disordered, poorly crystalline feitknechtite into fully crystalline manganite [17,35]. The mechanism underlying this phenomenon is unknown. Hypothetically, Mn^{2+} impurity (and, possibly, admixtures of other bivalent cations, e.g., Zn^{2+}) may stabilize the manganite structure. Taking into account the presence of a trace amount of a Mn^{2+} -bearing phase (rhodochrosite) in the manganite-related Zn,Mn-mineral from Kapova Cave, one can suppose that this mineral formed in accordance with a similar mechanism, from a birnessite-related mineral via an

intermediate feitknechtite phase. The morphological features of the mineral from Kapova Cave confirm this assumption. The mineral occurs as curved hexagonal lamellae (Figure 6), which is typical for feitknechtite, rather than manganite.

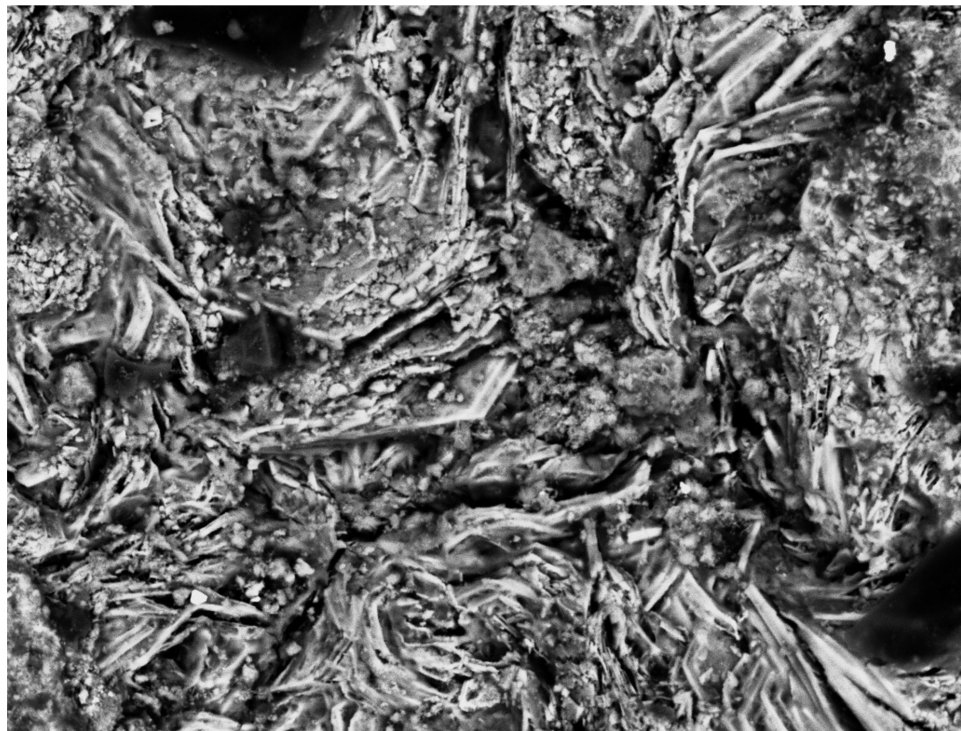


Figure 6. Aggregate of lamellae of the manganite-related Zn,Mn-mineral from Kapova Cave. SEM (BSE) image. Field of view width = 0.15 mm.

Thus, the existence of isostructural compounds or those that are closely related to each other in terms of structure with the general formula $(\text{Mn}^{3+}, \text{Mn}^{2+})\text{O}(\text{OH}, \text{H}_2\text{O})$, formed as a result of manganite reduction, cannot be excluded. It should be noted that the existence of so-called “manganous manganite” with the simplified formula $4\text{MnO}_2 \cdot \text{Mn}(\text{OH})_2 \cdot 2\text{H}_2\text{O}$ and a disordered structure was proposed by Feitknecht and Marti [24] based on powder XRD data.

As noted above, the 1×1 channels in the manganite-related structures are too small for the incorporation of H_2O molecules. Consequently, the bands of H_2O observed in the IR spectrum of the mineral from Kapova Cave may correspond to water molecules, substituting a part of the OH groups.

In conclusion, let us consider the problem of origin of the Zn,Mn-mineral from Kapova Cave. The cave is famous for its wall paintings of primitive people [43]. A number of sediment-hosted massive zinc-lead sulfide ore occurrences are situated in the Burzyansky district of Bashkortostan. The most famous of them is the Kuzha deposit ($53^\circ 15' 24''$ N, $57^\circ 10' 2''$ E) [44]. It can be assumed that the ZnMn hydroxide was brought from the oxidation zone of one of such ore occurrences by people of the Stone Age as a black pigment. However, this matter requires a separate serious investigation.

5. Conclusions

The three natural $\text{MnO}(\text{OH})$ polymorphs, namely, manganite, groutite, and feitknechtite, show different preferable mechanisms of coupled isomorphous substitutions involving Mn in different valence states and H-bearing species. The partial oxidation of groutite, a polymorph with tunnel structure that is isotypic with ramsdellite MnO_2 , results in the formation of so-called “groutellite”, $(\text{Mn}^{3+}, \text{Mn}^{4+})\text{O}(\text{OH}, \text{O})$, whereas groutite can be obtained in a reverse process of ramsdellite reduction. In groutite, OH groups form very

strong hydrogen bonds. Ramsdellite is nominally hydrogen-free, but in some ramsdellite samples the IR spectra indicate weak hydrogen bonds formed by OH groups.

The IR spectroscopic and XRD data show that there are two stages in the hydrolytic reduction of ramsdellite. One of these is accompanied by the formation of so-called “groutellite” as a result of partial protonation of the O2 atoms. “Groutellite” contains OH groups forming weak hydrogen bonds. Further protonation of O2 results in a phase transfer into a groutite-type compound, accompanied by a significant transformation of the framework and formation of strong hydrogen bonds. In both stages, the substitution of Mn^{4+} for Mn^{3+} takes place.

Manganite forms two solid-solution series: (1) with pyrolusite, forming oxy-hydroxides with the general formula $(\text{Mn}^{4+}, \text{Mn}^{3+})\text{O}(\text{OH}, \text{O})$, and (2) with a hypothetical structurally related compound $\text{ZnO}\cdot\text{H}_2\text{O}$, with the formation of hydrous oxy-hydroxides with the general formula $(\text{Mn}^{3+}, \text{Zn}^{2+})\text{O}(\text{OH}, \text{H}_2\text{O})$.

Feitknechtite is considered to be isostructural with (or structurally related to) the compounds $(\text{Mn}^{2+}, \text{Mn}^{3+})\text{O}(\text{OH}, \text{O})_2$, presumably formed in nature as intermediate phases during the rapid oxidation of pyrochroite. On the other hand, Mn^{2+} cations can promote the transformation of birnessite-type compounds with layered structures into manganite via an intermediate feitknechtite phase. Hypothetically, the mineral with the idealized formula $\text{Mn}^{3+}_{0.5}\text{Zn}^{2+}_{0.5}\text{O}(\text{OH})_{0.5}(\text{H}_2\text{O})_{0.5}$ from Kapova Cave is a product of the Zn- and/or Mn^{2+} -promoted transformation of a birnessite-related mineral via an intermediate feitknechtite-like phase. The existence of compounds with the general formula $(\text{Mn}^{3+}, \text{Mn}^{2+})\text{O}(\text{OH}, \text{H}_2\text{O})$, structurally related to manganite and formed as a result of manganite reduction, cannot be excluded.

Author Contributions: Conceptualization, N.V.C.; Methodology, N.V.C., D.A.V., N.V.Z., and S.N.B.; investigation, N.V.C., D.A.V., I.V.P., and S.N.B.; original manuscript draft preparation, N.V.C.; manuscript review and editing, I.V.P., D.A.V., A.V.K., and N.V.C.; figures, N.V.C. and D.A.V. All authors have read and agreed to the published version of the manuscript.

Funding: This work was performed in accordance with the state task, state registration no. AAA-A19-119092390076-7.

Acknowledgments: The authors thank the X-ray Diffraction Center of Saint-Petersburg State University for instrumental and computational resources.

Conflicts of Interest: The authors declare no conflict of interest.

References

1. Bhide, V.G.; Dani, R.H. Electrical conductivity in oxides of manganese and related compounds. *Physica* **1961**, *27*, 821–826. [[CrossRef](#)]
2. Giraldo, O.; Brock, S.L.; Willis, W.S.; Marquez, M.; Suib, S.L.; Ching, S. Manganese oxide thin films with fast ion-exchange properties. *J. Am. Chem. Soc.* **2000**, *122*, 9330–9331. [[CrossRef](#)]
3. Pasero, M. A short outline of the tunnel oxides. *Revs. Mineral. Geochem.* **2005**, *57*, 291–305. [[CrossRef](#)]
4. Crisostomo, V.M.B.; Ngala, J.K.; Alia, S.; Doble, A.; Morein, C.; Chen, C.-H.; Shen, X.; Suib, S.L. New synthetic route, characterization, and electrocatalytic activity of nanosized manganite. *Chem. Mater.* **2007**, *19*, 1832–1839. [[CrossRef](#)]
5. Odnovolova, A.M.; Sofronov, D.S.; Bryleva, E.Y.; Puzan, A.N.; Mateichenko, P.V.; Gudzenko, L.V.; Desenko, S.M.; Beda, A.A. Synthesis and properties of $\text{MnO}(\text{OH})$ particles. *Russ. J. Appl. Chem.* **2015**, *88*, 1440–1445. [[CrossRef](#)]
6. Byles, B.W.; Palapati, N.K.R.; Subramanian, A.; Pomerantseva, E. The role of electronic and ionic conductivities in the rate performance of tunnel structured manganese oxides in Li-ion batteries. *APL Mater.* **2016**, *4*, 046108. [[CrossRef](#)]
7. Bernardini, S.; Bellatreccia, F.; Della Ventura, G.; Ballirano, P.; Sodo, A. Raman spectroscopy and laser-induced degradation of groutellite and ramsdellite, two cathode materials of technological interest. *RSC Adv.* **2020**, *10*, 923–929. [[CrossRef](#)]
8. Gruner, J.W. Groutite, HMnO_2 , a new mineral of the diasporite-goethite group. *Am. Mineral.* **1947**, *32*, 654–659.
9. Glasser, L.S.D.; Ingram, L. Refinement of the crystal structure of groutite, $\alpha\text{-MnOOH}$. *Acta Cryst. B* **1968**, *24*, 1233–1236. [[CrossRef](#)]
10. Kohler, T.; Armbruster, T.; Libowitzky, E. Hydrogen bonding and Jahn-Teller distortion in groutite, $\alpha\text{-MnOOH}$, and manganite, $\gamma\text{-MnOOH}$, and their relations to the manganese dioxides ramsdellite and pyrolusite. *J. Solid State Chem.* **1997**, *133*, 486–500. [[CrossRef](#)]
11. Chabre, Y.; Pannetier, J. Proton intercalation in $\gamma\text{-MnO}_2$ from ramsdellite to groutite through groutellite. In *MRS Online Proceedings Library (OPL): Symposium U—Solid State Ionics IV*; Cambridge University Press: Cambridge, UK, 2011. [[CrossRef](#)]

12. Post, J.E.; Heaney, P.J.; Hanson, J.C. Temperature-resolved synchrotron X-ray diffraction study of ramsdellite and groutite. *Geol. Soc. Am. Ann. Meet. Boston* **2001**, *33*, 362–363.
13. Post, J.E.; Heaney, P.J. Neutron and synchrotron X-ray diffraction study of the structures and dehydration behaviors of ramsdellite and “groutellite”. *Am. Mineral.* **2004**, *89*, 969–975. [[CrossRef](#)]
14. Dachs, H. Neutronen- und Röntgenuntersuchungen am Manganit, MnOOH. *Z. Krist. Cryst. Mater.* **1963**, *118*, 303–326. (In German with English Abstract) [[CrossRef](#)]
15. Feklichev, V.G. *Diagnostic Constants of Minerals*; Nedra: Moscow, Russia, 1989; 479p. (In Russian)
16. Portehault, D.; Cassaignon, S.; Baudrin, E.; Jolivet, J.-P. Evolution of Nanostructured Manganese (Oxyhydr)oxides in Water through MnO₄⁻ Reduction. *Cryst. Growth Des.* **2010**, *10*, 2168–2173. [[CrossRef](#)]
17. Elzinga, E.J. Reductive transformation of birnessite by aqueous Mn (II). *Environ. Sci. Technol.* **2011**, *45*, 6366–6372. [[CrossRef](#)]
18. Yoshino, T.; Miura, H.; Hariya, Y. Crystal structure of orthorhombic pyrolusite from Imini Mine, Marrakesh, Morokko. In *Mineral Resources Symposia*; Soc. Resource Geologists Jap.: Tokyo, Japan, 1993; pp. 62–65.
19. Moore, T.P. Famous mineral localities: Ilfeld, Harz Mountains, Thuringia, Germany. *Mineral. Rec.* **2010**, *41*, 481–505.
20. Zhang, W.; Yang, Z.; Liu, Y.; Tang, S.; Han, X.; Chen, M. Controlled synthesis of Mn₃O₄ nanocrystallites and MnOOH nanorods by a solvothermal method. *J. Crystal Growth* **2004**, *263*, 394–399. [[CrossRef](#)]
21. Frondel, C. New manganese oxides: Hydrohausmannite and woodruffite. *Am. Mineral.* **1953**, *38*, 761–769.
22. Bricker, O. Some stability relations in the system Mn–O₂–H₂O at 25° and one atmosphere total pressure. *Am. Mineral.* **1965**, *50*, 1296–1354.
23. Nambu, M.; Tanida, K.; Kitamura, T.; Komura, T. Feitknechtite and its origin from Noda-Tamagawa mine, Iwate Prefecture, Japan. *Ganseki Kobutsu Kosho Gakkaishi J. Jpn. Assoc. Mineral. Petrol. Econ. Geol.* **1969**, *59*, 91–107. (In Japanese) [[CrossRef](#)]
24. Feitknecht, W.; Marti, W. Über Manganite and künstlichen Braunstein. *Helv. Chim. Acta* **1945**, *28*, 149–156. (In German) [[CrossRef](#)]
25. Yang, D.S.; Wang, M.K. Syntheses and characterization of well-crystallized birnessite. *Chem. Mater.* **2001**, *13*, 2589–2594. [[CrossRef](#)]
26. Wells, A.F. *Structural Inorganic Chemistry*, 4th ed.; Pergamon Press: Oxford, UK, 1973; pp. 520–528.
27. Meldau, R.; Newesley, H.; Strunz, H. Zur Kristallchemie von Feitknechtit, β-MnOOH. *Naturwissenschaften* **1973**, *60*, 387. [[CrossRef](#)]
28. Luo, J.; Segal, S.R.; Wang, J.Y.; Tian, Z.R.; Suib, S.L. Synthesis, characterization, and reactivity of feitknechtite. *Mat. Res. Soc. MRS Symp. Proc.* **1996**, *431*, 3–8. [[CrossRef](#)]
29. Peng, X.; Ichinose, I. Manganese oxyhydroxide and oxide nanofibers for high efficiency degradation of organic pollutants. *Nanotechnology* **2010**, *22*, 015701. [[CrossRef](#)] [[PubMed](#)]
30. Chukanov, N.V. *Infrared Spectra of Mineral Species: Extended Library*; Springer GmbH: Dordrecht, The Netherlands; Heidelberg, Germany; New York, NY, USA; London, UK, 2014; 1716p. [[CrossRef](#)]
31. Kulp, J.L.; Perfetti, J.N. Thermal study of some manganese oxide minerals. *Mineral. Mag.* **1950**, *29*, 239–250. [[CrossRef](#)]
32. Lima-de-Faria, J.; Lopes-Vieira, A. The transformation of groutite (α-MnOOH) into pyrolusite (MnO₂). *Mineral. Mag.* **1964**, *33*, 1024–1031. [[CrossRef](#)]
33. Libowitzky, E. Correlation of O–H stretching frequencies and O–H···O hydrogen bond lengths in minerals. *Monatshfte Chem.* **1999**, *130*, 1047–1059. [[CrossRef](#)]
34. Schwarzmann, E.; Glemser, O.; Marsmann, H. IR- und ¹H-Kernresonanzmessungen an InO(OH). *Z. Nat. B* **1966**, *21*, 1128–1131. (In German) [[CrossRef](#)]
35. Lefkowitz, J.P.; Rouff, A.A.; Elzinga, E.J. Influence of pH on the reductive transformation of birnessite by aqueous Mn (II). *Environ. Sci. Technol.* **2013**, *47*, 10364–10371. [[CrossRef](#)]
36. Lefkowitz, J.P.; Elzinga, E.J. Impacts of aqueous Mn(II) on the sorption of Zn(II) by hexagonal birnessite. *Environ. Sci. Technol.* **2015**, *49*, 4886–4893. [[CrossRef](#)] [[PubMed](#)]
37. Zhao, S.; González-Valle, Y.A.; Elzinga, E.J.; Saad, E.M.; Tang, Y. Effect of Zn(II) coprecipitation on Mn(II)-induced reductive transformation of birnessite. *Chem. Geol.* **2018**, *492*, 12–19. [[CrossRef](#)]
38. Schwarzmann, E.; Sparr, H. Die Wasserstoff-brückenbindung in Hydroxiden mit Diasporstruktur. *Z. Naturforsch.* **1969**, *24*, 8–11. (In German) [[CrossRef](#)]
39. Potter, R.M.; Rossman, G.R. The tetravalent manganese oxides: Identification, hydration, and structural relationships by infrared spectroscopy. *Am. Mineral.* **1979**, *64*, 1199–1218.
40. Fleischer, M.; Richmond, W.E.; Evans, H.T., Jr. Studies of the manganese oxides V. Ramsdellite, MnO₂, an orthorhombic dimorph of pyrolusite. *Am. Mineral.* **1962**, *47*, 47–57.
41. Grangeon, S.; Warmont, F.; Tournassat, C.; Lanson, B.; Lanson, M.; Elkaïm, E.; Claret, F. Nucleation and growth of feitknechtite from nanocrystalline vernadite precursor. *Eur. J. Mineral.* **2017**, *29*, 767–776. [[CrossRef](#)]
42. Hem, J.D.; Roberson, C.E.; Fournier, R.B. Stability of β-MnOOH and manganese oxide deposition from springwater. *Water Resour. Res.* **1982**, *18*, 563–570. [[CrossRef](#)]
43. Lawson, A.J. *Painted Caves: Palaeolithic Rock Art in Western Europe*; Oxford University Press: Oxford, UK, 2012; 456p, ISBN 978-0-19-969822-6.
44. Filippov, V.A. The Kuzha barite–base-metal deposit. *Geol. Ore Depos.* **2008**, *50*, 391–403. [[CrossRef](#)]